

Assessment of Central Retinal Function in Patients with Advanced Retinitis Pigmentosa

Christina Gerth, Tom Wright, Elise Héon, and Carol A. Westall

PURPOSE. To assess central retinal function in patients with advanced retinitis pigmentosa (RP) using the multifocal (mf)ERG and static perimetry.

METHODS. Patients with RP; a nonrecordable, full-field (ff)ERG; and visual acuity (VA) of ≤ 1.0 logMAR were included. All patients underwent mfERG testing (103 hexagons, and 2.67 and 5.33 $\text{cd} \cdot \text{s} \cdot \text{m}^{-2}$ flash intensities) and static perimetry (103 corresponding areas) in the better eye. First-order kernel mfERGs were analyzed for total noise, signal-to-noise ratio, response amplitude, and implicit time. The number of areas with recordable mfERG responses were counted and compared with visual field (VF) sensitivity.

RESULTS. Twenty-nine patients aged 16 to 68 years with a VA of 0.02 to 1.0 logMAR and a kinetic VF of 10° to 60° in diameter were included. mfERGs were successfully performed in 22 of 29 patients. Responses were detected in at least one stimulated area in 22 of 22 patients, with an overall response detection of 9.8% in all stimulated areas and no difference between flash intensities. All responses were diminished severely in response density P1-N1, with normal P1 implicit time in 50% of the recordings. No predictive factors for recordable mfERG responses were identified. VF results were recorded reliably in 27 of 29 patients, with a 40% response detection rate.

CONCLUSIONS. mfERG responses were recordable in at least one area in all successfully tested patients with advanced RP. Response detection and performance was significantly higher for static perimetry. Static perimetry may be a more sensitive primary outcome measure of central vision function than the mfERG in patients with advanced RP and nonrecordable ffERGs. (*Invest Ophthalmol Vis Sci.* 2007;48:1312-1318) DOI: 10.1167/iovs.06-0630

Retinitis pigmentosa (RP) refers to a group of hereditary retinal degenerations with a prevalence of approximately 1 in 4000.¹ Characteristic symptoms include nyctalopia, impaired dark adaptation, and a progressive visual field loss that often leads to legal blindness.^{2,3} Advanced RP is characterized by a nonrecordable full-field (ff)ERG and a severely constricted visual field of less than 20° , but often well-preserved central

vision.⁴ It has been shown that static visual field (VF) testing is a sensitive tool to quantify this preserved central VF in this patient population.⁵⁻⁸ The VF test, however, has limitations: (1) as a behavioral method, the response may undergo signal modulation and processing within the retinal and cortical visual pathway⁹; (2) the test is subjective in nature and relies on the patient's cooperation and experience with the test. Electrophysiological tests, in contrast, are objective measures of retinal function. The origin of the ffERG (reviewed in Ref. 10) and multifocal (mf)ERG¹¹ responses has been correlated to distinct retinal layers and can indicate the point of cellular dysfunction. The ffERG is often nonrecordable above noise in patients with advanced diseases,^{3,12} except when using specific signal acquisition and filtering techniques.¹³⁻¹⁵ The mfERG technique developed by Sutter and Tran^{16,17} permits a localized measurement and mapping of the retinal response. The cone-mediated mfERG with localized retinal stimulation may allow quantification of the remaining cone-mediated function, despite an advanced stage of disease.¹⁸⁻²³ This may be particularly useful in characterizing better advanced stages of disease. Several studies involving patients with RP and Usher syndrome with either recordable or nonrecordable ffERG responses suggest that the mfERG allows a quantification of the central cone-mediated function.¹⁸⁻²⁴ Validation of arising treatment options will require reliable outcome measures to quantify retinal function.²⁵

The objectives of our study were (1) to assess the central retinal responses in patients with advanced RP and a nonrecordable ffERG (International Society for Electrophysiology of Vision [ISCEV] standard),²⁶ by using the cone-mediated mfERG, and (2) to compare the mfERG sensitivity with static perimetry in those patients.

In the population tested, we identified mfERG responses in less than 10% of stimulated areas in 76% of the patients tested. Recordable mfERGs exhibited a greater reduction in amplitude than delay in implicit time. No predictive factors for an acceptable signal-to-noise response were identified. The static visual field test was more sensitive in detecting remaining central retinal responses than was the mfERG.

MATERIALS AND METHODS

Subjects

Participants were recruited from the Ocular Genetics Clinic at The Hospital for Sick Children. Written informed consent was obtained from all participants or their guardians in accordance with the tenets of the Declaration of Helsinki. The project was approved by the Research Ethics Board of the Hospital for Sick Children, Toronto. Inclusion criteria were diagnosis of syndromic or nonsyndromic RP² with nonrecordable ffERG (ISCEV standard²⁶), visual acuity (VA) in the better eye of 1.0 logMAR or better, an interpretable Goldmann visual field (test target III_{4c}) and the ability to perform the proposed tests. Exclusion criteria were significant media opacities; cystoid macula edema (visualized by ophthalmoscopy and/or optical coherence tomography); or the presence of a maculopathy, glaucoma, nystagmus, myopia greater than -6.00 DS (which could interfere with mfERG responses²⁷).

From the Department of Ophthalmology and Vision Sciences, The Hospital for Sick Children and University of Toronto, Toronto, Ontario, Canada.

Supported by the Sick Kids Research Institute's Restracom Fund (CG), The Foundation Fighting Blindness/Canada (EH), and The Juvenile Diabetes Research Fund (mfERG analysis: CAW).

Submitted for publication June 9, 2006; revised August 3, October 2, and November 1, 2006; accepted January 5, 2007.

Disclosure: C. Gerth, None; T. Wright, None; E. Héon, None; C.A. Westall, None

The publication costs of this article were defrayed in part by page charge payment. This article must therefore be marked "advertisement" in accordance with 18 U.S.C. §1734 solely to indicate this fact.

Corresponding author: Carol A. Westall, Department of Ophthalmology and Vision Sciences, The Hospital for Sick Children and University of Toronto, 555 University Avenue, Toronto, ON, M5G 1X8, Toronto, Canada; carol@sickkids.ca.

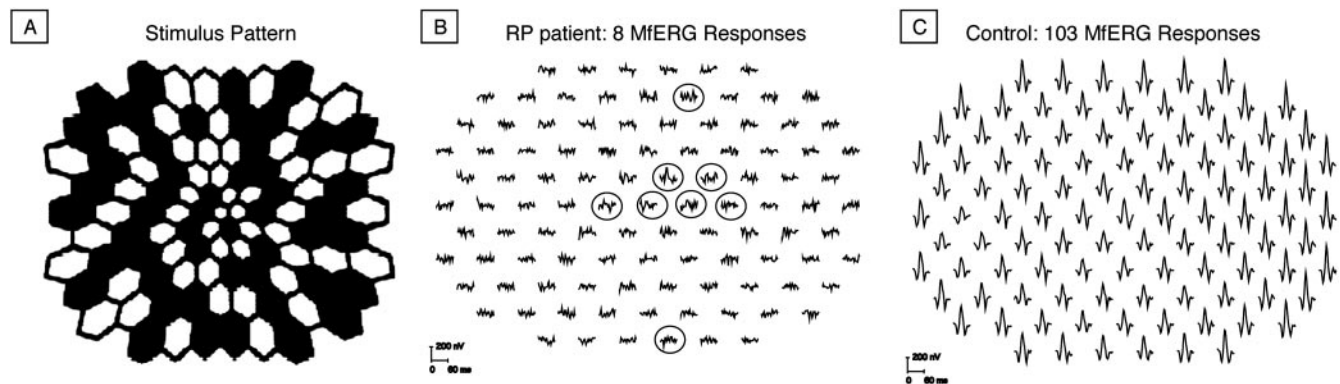


FIGURE 1. mfERG stimulus array with 103 hexagons (A). Typical response examples of patient 1 (B) and the mean of an age-matched control group (C) at a stimulus intensity of $200 \text{ cd} \cdot \text{m}^{-2}$ are shown. *Circled* mfERGs in (B) reflect responses above noise in the patient's recording.

or any systemic (e.g., diabetes) or neurologic diseases that could affect vision or the capacity to perform the tests.

Vision Function Assessment

Best-corrected distance VA was assessed on a logMAR (logarithm of the minimum angle of resolution) scale by using the backlit Early Treatment Diabetic Retinopathy Study charts (ETDRS).²⁸ Contrast sensitivity (CS) was measured using the Pelli-Robson Contrast Sensitivity charts at a 1-meter distance.²⁹ Slit-lamp examination and intraocular pressure measurement were performed in all patients before testing. Goldmann visual fields were repeated if they had not been performed within the previous 6 months. The index eye was (1) the eye with the better VA, (2) the eye with the better CS in patients with equal VA in both eyes, or (3) a randomly chosen eye in patients with equal VA and CS in both eyes.

Multifocal ERG

Stimulation and primary analysis were performed using a stimulus-camera-refractor unit (VERIS, ver. 5.1; Electrodiagnostic Imaging [EDI] San Mateo, CA). After full pupil dilation, mfERGs were recorded from the index eye with a bipolar Burian-Allen contact lens electrode with a built-in infrared illuminator (Hansen Ophthalmic Development Laboratory, Coralville, IA, and EDI) placed on the corneal surface of the eye. Refractive errors were corrected by using the built-in refractor unit. The stimulus consisted of 103 scaled hexagons extending 20° in radius flashed in a pseudorandom pattern at intervals of 13.3 ms (m-sequence-length, $2^{15} - 1$) on a dark background ($<1 \text{ cd} \cdot \text{m}^{-2}$), as illustrated in Figure 1A.

A pilot study was undertaken in a similar patient group that indicated that a maximum flash intensity of $5.33 \text{ cd} \cdot \text{s} \cdot \text{m}^{-2}$ ($400 \text{ cd} \cdot \text{m}^{-2}/75 \text{ Hz}$), as used by Hood et al.,¹⁹ might result in a higher number of retinal responses than a lower flash intensity (lower luminance). To confirm this, each patient was tested twice, first at a maximum flash intensity of $2.67 \text{ cd} \cdot \text{s} \cdot \text{m}^{-2}$ ($200 \text{ cd} \cdot \text{m}^{-2}/75 \text{ Hz}$) and consecutively at $5.33 \text{ cd} \cdot \text{s} \cdot \text{m}^{-2}$ at a high contrast of 99% and adjusted surround of 50%. Signals were sampled at 1200 Hz (i.e., 0.83 ms between samples). The data were acquired at a gain of 50,000 over a frequency range of 10 to 300 Hz (preamplifier model ICP 511; Grass Telefactor, West Warwick, RI). Stable fixation was achieved displaying a black fixation cross 4° in diameter with a pen size of 20%, which covers less than 40% of the central hexagon and less than 10% of the adjacent hexagons. Stimulus luminance was calibrated with the auto-calibrator (EDI).

The total duration of the m-sequence used was 7 minutes 17 seconds and was divided into 16 segments of 27.29 seconds each. Steady fixation was ensured by viewing the fundus with a built-in infrared fundus camera. The criteria for repeating a segment were movements and/or saccades exceeding 3° or the size of the optic disc. Such movements usually did not exceed two to four times during each

recording. Recorded segments with physiological saccades with immediate refixation were not excluded.

The protocol followed the recommended guidelines of the International Society for Electrophysiology of Vision (ISCEV) for basic mfERG, with the addition of the variable luminance.³⁰

Central Visual Fields

Static central visual fields were assessed with the Humphrey Visual Field Analyzer (HFA II; Carl Zeiss Meditec, Inc., Dublin, CA) using a customized program (Humphrey Visual Field; HVF).^{19,24} The perimeter display was customized to match the mfERG test pattern. Thresholds were measured at 103 locations with a size 3, white test stimulus centered in the middle of each hexagonal area and the SITA protocol. The background illumination was $10 \text{ cd} \cdot \text{m}^{-2}$. Full refractive correction was used. Eye and head tracking was monitored. Each patient was given 1-minute breaks every 3 to 4 minutes of testing to ensure alertness.

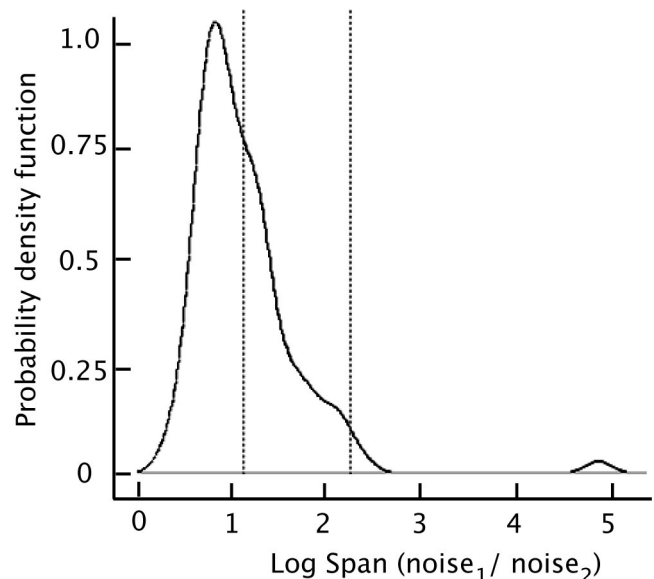


FIGURE 2. Distribution of noise estimates in control subjects followed a normal distribution. Vertical lines illustrate the mean and 2 SD from the mean. Patients' mfERG with noise estimated exceeding the 95th percentile of the control noise estimate were rejected and excluded from further analysis.

TABLE 1. Summary of Visual Function Test Results

Dx	Patient (n/Sex/Age)	VA (LogMAR)	CS (Log Units)	GVF (III _{4c}) Diameter (°)	HVF counts	mfERG Counts 200/400	mfERG: RD P1-N1 200/400 (nV/deg ⁻²)	mfERG: IT P1 200/400 (ms)
ADRP	1/m/27	0.02	1.5	25	87	8/3	14.4/3	25/26.7
ADRP	2/f/57	0.22	1.05	15	33	No fix	NA	NA
ADRP	3/f/54	0.4	1.05	30	39	12/noise	3.3/NA	43.3†/NA
ARRP	4/m/16	0.3	1.25	10	24	5/5	2.6/5.7	31.6†/33.3†
ARRP	5/m/30	0.64	0.45	20*	26	No fix	NA	NA
XLRP	6/m/21	0.1	1.20	20	88	6/10	10.3/3.3	22.5/26.6
XLRP	7/f/49	0.28	1.05	20	37	8/4	1.4/2.8	31.6†/25
XLRP	8/m/23	0.4	1.25	20	58	21/23	3.3/2.5	23.3/29.1†
sRP	9/m/41	0.05	1.5	60	42	19/5	3.1/25.7	26.6†/27.5†
sRP	10/m/49	0.1	1.2	20	27	Noise/9	NA/2.1	NA/30.8†
sRP	11/m/37	0.1	1.20	25	60	6/13	3.3/5.5	26.6†/29.1†
sRP	12/m/46	0.1	1.45	25	48	8/13	2.7/1.5	26.6†/24.9
sRP	13/m/27	0.1	1.35	45	UR	11/33	15.5/13.6	30.0†/27.5†
sRP	14/m/43	0.6	0.3	15	42	Noise/11	NA/3.0	NA/26.7†
sRP	15/f/37	0.4	1.25	20	32	8/10	2.4/4.8	25.8/30.8†
sRP	16/f/40	0.4	1.1	20	65	Noise	NA	NA
sRP	17/f/34	0.42	1.65	35*	103	Noise	NA	NA
sRP	18/f/68	0.5	0.6	10	7	11/4	2.6/2.4	28.3/27.5
sRP	19/f/48	0.52	0.75	40	69	9/17	3.7/3.2	25.8/24.9
sRP	20/m/50	0.64	0.6	10	6	No fix	NA	NA
sRP	21/m/35	1.0	0.15	20*	UR	3/9	1.8/9.1	36.6†/27.7
CHM	22/m/47	0.3	1.35	20*	35	Noise/6	NA/1.8	NA/25.8
USH 1	23/m/48	0.1	1.65	15	17	11/9	3.8/5.7	21.7/23.3
USH 1	24/m/35	0.26	1.3	20	36	No fix	NA	NA
USH 2	25/m/43	0.16	1.5	25	46	10/14	7.5/4.9	26.7†/24.2
USH 2	26/f/41	0.1	1.55	10*	18	6/3	4.6/3.3	26.6†/24.1
USH 2	27/f/34	0.1	1.55	20	54	6/10	6.7/5.7	30†/24.1
USH 2	28/f/47	0.3	1.45	35	83	16/noise	8.2/NA	25.8/NA
USH 3	29/m/52	0.22	1.15	10	6	No fix	NA	NA

Counts refer to an area with measurable HVF threshold/mfERG responses. RD, response density; IT, implicit time; ADRP, autosomal-dominant RP; ARRP, autosomal-recessive RP; sRP, simplex RP; USH, Usher syndrome; CHM, choroideremia; NT, not tested; UR, unreliable; no fix, not able to see fixation target or test stimulus; NA, not applicable; VA, visual acuity; CS, contrast sensitivity; GVF, Goldman visual field; mfERG, multifocal electroretinogram (tested at 200 and 400 cd · m⁻²); HVF, Humphrey visual field.

* Plus peripheral visual field island.

† Implicit time delay >2 SD.

Response Analysis

Two iterations of artifact rejection, but no spatial averaging was applied to the raw mfERG data. mfERGs were analyzed for noise to exclude poor-quality recording as follows. The root mean square (RMS) of a higher-order kernel without a signal correlation was measured as a total noise estimate and compared with an already established control dataset ($n = 150$). The control noise estimate approximately follows a normal distribution, as shown in Figure 2. mfERG data with a noise estimate larger than the 95th percentile of the control dataset were excluded from further analysis.

Two different analyses, the signal-to-noise ratio (SNR) analysis and the stretch-fit analysis described by Hood and Li,³¹ were applied

to identify the more powerful method able to extract the expected small responses. (1) SNR analysis: First-order kernel responses were extracted from the epoch lengths 0 to 60 ms (signal-S), 60 to 120 ms (noise₁), and 120 to 180 ms (noise₂). (The late-epoch window of the first-order kernel response was a more stringent noise estimator than the fourth-order kernel, when applied to the SNR analysis in our patient cohort.) Waveform analysis was performed with custom software written in R.³² Responses with a low SNR may be caused either by high noise or low signal. It is very likely that RP-associated cone-mediated dysfunction will cause a low signal. Therefore, the noise ratio noise₁/noise₂ was calculated as an indicator for noise distribution for each individual recording. The SNR for each indi-

TABLE 2. Results of mfERG and HVF Performance and Response Count

Test	Patients <i>n</i> (%)	Patient Age (y)	Identified Response Number per Patient (max 103)
mfERG successfully performed (200 cd · m ⁻² and 400 cd · m ⁻²)	24/29 (83%)	18–57 (mean 42)	
mfERGs within noise limit			
200 cd · m ⁻²	19/24 (79%)	14–68 (mean 37)	3–21 (mean 9.7)
400 cd · m ⁻²	20/24 (83%)	14–68 (mean 37)	3–33 (mean 11.0)
mfERGs exceeding noise limit:			
200 cd · m ⁻²	5/24 (21%)	34–49 (mean 43)	NA
400 cd · m ⁻²	4/24 (17%)	34–54 (mean 44)	NA
HVF successfully performed	27/29 (93%)	14–68 (mean 40)	5–103 (mean 41)

vidual mfERG was calculated by the quotient of S/noise_2 . Responses were deemed detectable if the SNR was greater than the mean noise ratio + 1.96 SD. (More details are described in the Appendix.) (2) Stretch-fit analysis: Response templates from age-matched control subjects were created for each hexagon. Templates were stretched in both time and amplitude to obtain the best fit with a noise window (120–180 ms epoch) from the patient's recording to build a distribution of template fits for each patient achieved randomly. Templates were then refitted to the signal components of each patient's recording (0–60 ms epoch). Responses were considered detectable if hexagons achieved a fit greater than the mean noise fit + 1.96 SD.

Responses of each recording were counted, and response density P1-N1 and implicit time P1 were compared with age-matched control subjects ($n = 26$; ages, 13–51 years).

HVF tests with a fixation loss of less than 20% and false-positive or false-negative responses less than 33% were reliable and included in the analysis. HVF responses were counted for each patient. The number of detectable mfERG and HVF responses was compared, to identify which was the more sensitive test procedure in this patient cohort.

Clinical test results such as VA, CS, Goldmann visual field, age at testing or RP type were analyzed and correlated with the number of identified hexagons by using a one-way ANOVA for categorical variables and Spearman test.³²

RESULTS

General Findings

Twenty-nine patients (11 female and 18 male) aged 16 to 68 years (mean, 40) were included in the study. Diagnoses included RP ($n = 21$), choroideremia ($n = 1$), or Usher syndrome ($n = 7$). Heritance in patients with RP was autosomal dominant (3/29), autosomal recessive (2/29), or X-linked (3/29) or was categorized as simplex RP (13/29). Simplex RP refers to cases where only one member of the family (the patient tested) is affected and no other inheritance clues, such as mutations or carrier stage have been found in other family members.

Visual acuity ranged from 0.05 to 1.0 logMAR (mean, 0.3). Contrast sensitivity was reduced in 23 of 29 patients with a range of 1.65 to 0.15 log units (mean, 1.15). Kinetic visual fields were constricted from 10° to 60° in diameter (mean, 23°). Thirteen of 29 patients had been tested with the HVF or with a different static perimetry test at one time during the disease course, between 1.15 and 13 years before this study (mean, 3.6 years). Demographic data and vision function results are summarized in Table 1.

Multifocal ERG

Figure 1 shows a typical example of a patient recording compared with that of a control subject. Eighty-three percent of patients were able to perform the test. Five patients could not see the fixation target or even the test stimulus itself. Age, kinetic visual field size, VA, and CS were not different in those 5 patients compared with the other 34 patients.

Data from five recordings at $200 \text{ cd} \cdot \text{m}^{-2}$ and four recordings at $400 \text{ cd} \cdot \text{m}^{-2}$ in a total of seven patients, were excluded from further analysis because of a large total noise estimate. Data from two of the seven patients exceeded the noise level for both intensities. The other five patients had a noise-acceptable mfERG for one of the stimulus intensities. The resultant 39 recordings from 22 of 29 patients (19 recordings at $200 \text{ cd} \cdot \text{m}^{-2}$ and 20 at $400 \text{ cd} \cdot \text{m}^{-2}$), were analyzed for responses in each of the 103 stimulated areas.

Analyses Comparison

The SNR analysis and the stretch-fit analysis method were not significantly different in response identification ($200 \text{ cd} \cdot \text{m}^{-2}$: $P = 0.39$; $400 \text{ cd} \cdot \text{m}^{-2}$: $P = 0.27$, paired *t*-test). The localization of identified mfERG responses identified by the two analysis methods did not correlate significantly ($P = 0.25$, McNemar's test). Averaged waveforms from identified responses were generated for each patient by each method. These waveforms were compared with template waveforms from the same hexagons in age-matched control subjects using a measure of correlation suggested by Woody.³³ The SNR analysis showed a significantly better correlation with age-matched control tem-

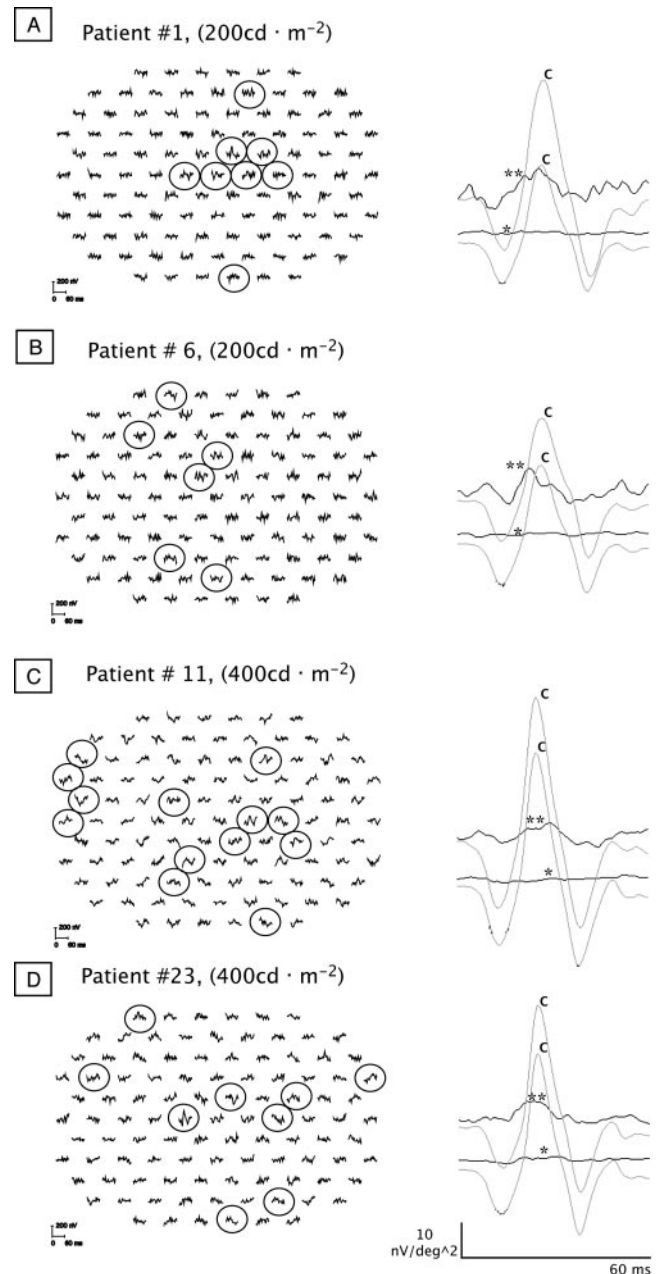


FIGURE 3. Examples of mfERG signals for patients 1 (A), 6 (B), 11 (C), and 23 (D). mfERG responses are circled in the mfERG traces array. The averages of the mfERG with identified responses (**) and without identified responses (*) are plotted against the age-matched control of the corresponding areas (C, thinner traces).

TABLE 3. Correlation of mfERG Counts

	mfERG Counts (200 cd · m ⁻²)
Age	0.15
Diagnosis*	0.26
Visual acuity	-0.12
Contrast sensitivity	0.26
Goldmann visual field	0.50†

Data are Spearman *r*. Counts refer to an area with measurable mfERG responses.

* F statistic.

† *P* = 0.03, but considered as not significant, because applied Bonferroni adjustment.

plates (*P* = 0.04, paired *t*-test) than did the stretch-fit analysis in this patient population. We decided, therefore, that the SNR analysis was more suitable for this patient population and we applied it to each of the single mfERGs.

Response Identification

Responses were identified in 9.8% (395/4017) of the stimulated areas. There was no statistically significant sensitivity difference between the two stimulus intensities (*P* > 0.05, Wilcoxon rank sum test); 184 of 1957 signals (103 stimulated areas × 19 recordings) and 211 of 2060 signals (103 stimulated areas × 20 recordings) were identified as detectable responses for the 200 cd · m⁻² and 400 cd · m⁻² stimulus condition, respectively (Table 2).

Typical examples of the response analysis are shown in Figure 3. Identified mfERG responses are encircled in each of the trace plots. The number of identified responses range from 7 to 13 of the 103 areas stimulated in these four examples. The response average P1 implicit time was within normal limits in patients 1, 6, and 23 and delayed by 3.7 SD in patient 11. The age-matched control response in the corresponding areas (gray traces) illustrates the extent of response reduction in the patient group.

None of the studied parameters, such as patients' age, RP type, VA, CS, or kinetic visual field size, correlated with the number of detectable mfERG responses (Table 3).

mfERG Comparison with Control Data

Responses were not analyzed from each hexagon individually because the very small response SNRs do not allow accurate implicit time and response density scoring. Therefore, identified mfERG responses were averaged for each of the subject's

recordings and compared with age-matched control data from topographically identical hexagons. Figure 4 illustrates the extent of implicit time delay and response density reduction compared with control data. The mean decrease in response density was 3.6 SD with only 14% of recordings falling within the 95th percentile confidence limits of control data. The average of the detectable responses exceeded 10 μV/deg² in only 5 of 39 recordings (each of the localized 103 responses in a control subject was larger than 10 μV/deg²). P1 implicit times were within normal range in 39% and 59% for the 200-cd · m⁻² and 400 cd · m⁻² stimulus condition, respectively. Nine responses were delayed >5 SD.

Central Visual Field Comparison with the mfERG

The test performance of the HVF was better than the mfERG. All but two patients were tested successfully with the HVF. Results from those two patients were excluded from the analysis because of the large number of false-positive and -negative responses, which were due to obvious reduced compliance during the test. Both of them had an mfERG recorded successfully. Visual field responses were detected in 40% of the tested areas (5–103; mean 41 areas) in 27 patients tested successfully.

Data from patients with both mfERG and HVF results were compared. The HVF test was significantly more sensitive than the mfERG in detecting localized responses (*P* < 0.001, paired *t*-test).

HVF sensitivity was significantly higher in areas with detectable mfERG responses than in areas without them (*P* = 0.003, 200 cd · m⁻²; *P* = 0.04, 400 cd · m⁻²; Welch two-sample *t*-test) as illustrated in Figure 5. A correlation between the mfERG and the HVF test was found in areas with measurable responses (*P* < 0.001; McNemar test). Therefore, mfERG responses were most likely found in areas with identified HVF responses.

DISCUSSION

Sensitive and reliable outcome measures are necessary to characterize the natural disease history and are fundamental in monitoring disease outcome. Electrophysiological tests, such as the scotopic and photopic full-field ERG, are objective and reliable measures to quantify overall retinal function.^{13,25} In patients with advanced RP, photoreceptor and inner retinal layer function may be too small to be measurable by the full-field ERG (ISCEV standard²⁶). We expected that the mfERG would be sensitive enough to quantify the cone-mediated function in most of the patients who had advanced RP and preserved central vision. Hence, we postulated that the mfERG

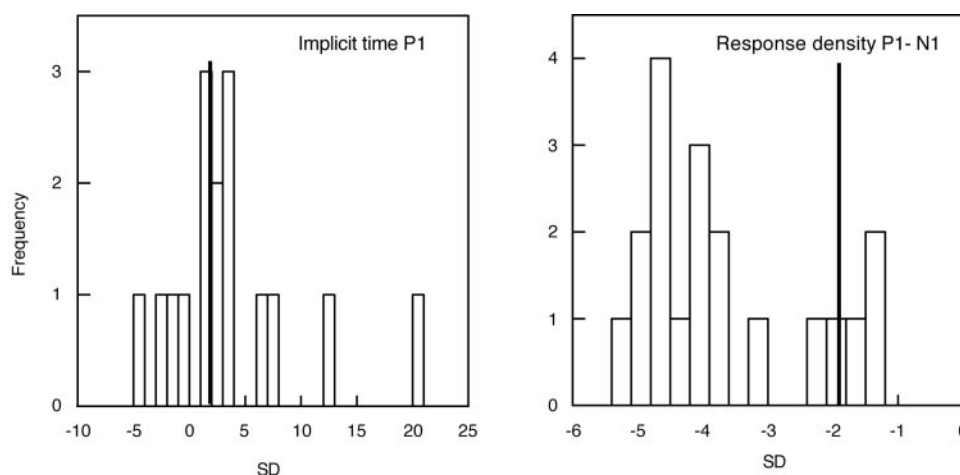
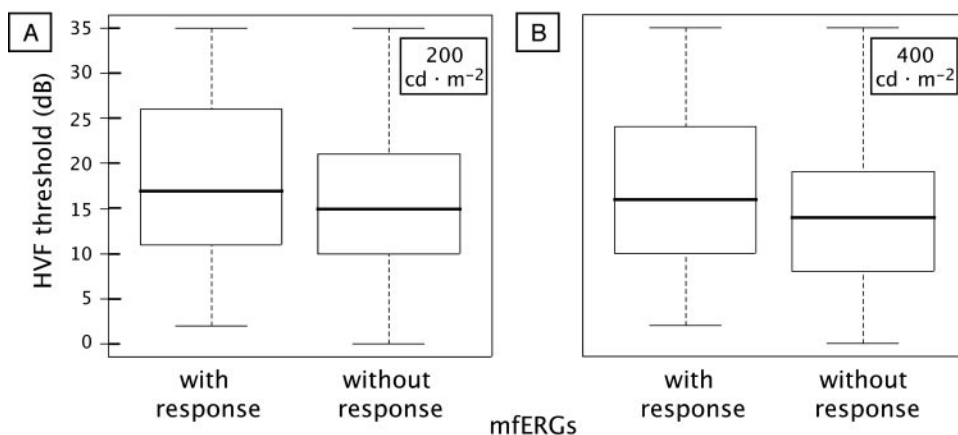


FIGURE 4. Comparison of the mfERG response implicit time P1 (A) and response density P1-N1 (B) with age-matched control are plotted for the stimulus intensity 200 cd · m⁻² in a histogram. The number of patients is plotted as a function of standard deviations from age-matched control data. Bold line: the point of significantly abnormal data (>2 SD).

FIGURE 5. Humphrey visual field (HVF) threshold average plotted for tested mfERG areas with responses and with noise for the two test conditions: (A) $200 \text{ cd} \cdot \text{m}^{-2}$ and (B) $400 \text{ cd} \cdot \text{m}^{-2}$. Boxes enclose 50% of the data with the median value displayed as a line; the tops and bottoms of the boxes mark 25%; and the error bars denote the minimum and maximum values of the data set. HVF averaged threshold was significantly different in areas with and without mfERG responses. ($P = 0.003$; $200 \text{ cd} \cdot \text{m}^{-2}$; $P = 0.04$, $400 \text{ cd} \cdot \text{m}^{-2}$, Welch two-sample *t*-test).



could be used as an outcome measure in further studies involving those patients with advanced retinal disease.

Previous studies assessing the applicability of the mfERG technique in patients with RP used different recording and analysis protocols, applied different inclusion criteria, and tested different RP subtypes than the present study.^{18–24} Signal-to-noise differentiation is crucial in the determination of detectable small-amplitude responses, which may not always be applied in the previous studies. Hood et al.¹⁹ successfully tested eight patients with RP, who had larger visual fields than those recorded in patients in the present study, and all but one had a recordable ffERG. They concluded that the total mfERG response depends on the relative size of the peripheral mfERG response. Seeliger et al.¹⁸ concluded that mfERG responses are nonrecordable in patients with RP with a Goldmann visual field of $<10^\circ$ and a photopic full-field 30-Hz flicker response of $1 \mu\text{V}$ or less. The present study shows that at least one response is recordable in all successfully tested patients using an objective signal-to-noise analysis paradigm, irrespective of the kinetic visual field size. We were able to identify responses even in patients with restricted kinetic visual fields smaller than 10° in radius. Severely diminished responses were associated with normal temporal characteristics in nearly 50% of the responses, which agrees with the findings of Hood et al.¹⁹ What is somewhat surprising is the finding that some patients lacked a central mfERG response despite a visual acuity of 0.4 logMAR or better and a normal HVF foveal threshold. Seiple et al.³⁴ showed a similar example of a patient with RP, VA of 20/25, and preserved mfERG responses in the peripheral area without a central response. In such cases, the number of intact photoreceptors may be sufficient to resolve a small visual angle required for good VA. The mfERG, on the one hand, may not be sensitive enough to detect signals initiated by the same amount of photoreceptors. Static perimetry, on the other, is a threshold test with a higher sensitivity range due to cortical amplification.

The mfERG may not be recommended as a primary outcome measure in patients with advanced RP and nonrecordable ffERG. Three critical observations were made in this specific patient group: (1) Response identification was positive in only 10% of all areas tested; (2) 17% of the patients were not able to perform the mfERG, despite high motivation and cooperation. These patients did not differ in age, visual acuity, contrast sensitivity or visual field size from patients who were able to perform the test. A conventional screen presentation may facilitate localizing the stimulus by the patient, but at the expense of monitoring fundus fixation. This compromise, we believed, would not be acceptable; (3) test compliance and success rate were higher with static perimetry than the with

mfERG test in this specific patient cohort. Signal exceeded the expected noise level in 15% of the mfERG recordings, which may be caused by undetected fixation instability during recording. The static visual field test, in contrast, was more sensitive in detecting central retinal function in the same patients. There may be a bias due to previous experience with the test procedure in less than 50% of our patients. The long period since the previous static visual field in respect to changed visual perception due to disease progression makes it unlikely that this preexistent experience interferes with the results in our study. The heterogeneous and not yet identified genotype in our patient cohort may be a factor for response detection. However, those patients are all tested at an advanced stage of disease with the same inclusion criteria.

Small-amplitude mfERG responses are detectable in all successfully tested patients with advanced RP, using the described analysis method. However, static perimetry provides a better functional outcome measure of central visual function when compared with the mfERG in this advanced stage of disease. Both tests remain useful as a baseline measure in patients with advanced RP nonrecordable ffERGs. If the carefully performed mfERG analysis, including the signal-to-noise analysis fails to detect responses in the tested area, the central static perimetry would be a measure suitable for longitudinal studies of residual function using the patient's individual reliability.³⁴ The use of both tests in patients with recordable mfERG responses may be beneficial in assessing longitudinal dynamics of retinal dysfunction with disease progression or in quantifying outcome.

Acknowledgments

The authors thank Yesmino Elia for coordinating the study, Rita Buffa for technical assistance, Alex Levin for patient recruitment, and Carole Pantone for editorial comments.

References

- Berson EL. Retinitis pigmentosa. The Friedenwald Lecture. *Invest Ophthalmol Vis Sci.* 1993;34:1659–1676.
- Heckenlively JR. *Retinitis Pigmentosa*. Philadelphia: JB Lipincott; 1988.
- Weleber R. Retinitis pigmentosa and allied disorders. In: Ryan S, editor. *Retina*. 2nd ed. St. Louis, MO: Mosby; 1994:335–466.
- Grover S, Fishman GA, Anderson RJ, Alexander KR, Derlacki DJ. Rate of visual field loss in retinitis pigmentosa. *Ophthalmology.* 1997;104:460–465.
- Lodha N, Westall CA, Brent M, Abdolell M, Heon E. A modified protocol for the assessment of visual function in patients with retinitis pigmentosa. *Adv Exp Med Biol.* 2003;533:49–57.

6. Swanson WH, Feliuss J, Birch DG. Effect of stimulus size on static visual fields in patients with retinitis pigmentosa. *Ophthalmology*. 2000;107:1950-1954.
7. Abe K, Iijima H, Hirakawa H, Tsukahara Y, Toda Y. Visual acuity and 10 degrees automated static perimetry in eyes with retinitis pigmentosa. *Jpn J Ophthalmol*. 2002;46:581-585.
8. Jacobson SG, Voigt WJ, Parel JM, et al. Automated light- and dark-adapted perimetry for evaluating retinitis pigmentosa. *Ophthalmology*. 1986;93:1604-1611.
9. Walraven J, Enroth-Cugell C, Hood DC, MacLeod DIA, Schnapf JL. The control of visual sensitivity: receptor and postreceptor processes. In: Spillmann L, Werner JS, ed. *Visual Perception. The Neurophysiological Foundations*. San Diego: Academic Press; 1990:53-101.
10. Frishman LJ. Origins of the electroretinogram. In: Heckenlively JR, Arden GB, eds. *Principles and Practice of Clinical Electrophysiology of Vision*. Cambridge, MA: MIT; 2006:139-183.
11. Hood DC, Frishman LJ, Saszik S, Viswanathan S. Retinal origins of the primate multifocal ERG: implications for the human response. *Invest Ophthalmol Vis Sci*. 2002;43:1673-1685.
12. Birch DG, Anderson JL, Fish GE. Yearly rates of rod and cone functional loss in retinitis pigmentosa and cone-rod dystrophy. *Ophthalmology*. 1999;106:258-268.
13. Birch DG. Surrogate electroretinographic markers for assessing therapeutic efficacy in the retina. *Expert Rev Mol Diagn*. 2004;4:693-703.
14. Andreasson SO, Sandberg MA, Berson EL. Narrow-band filtering for monitoring low-amplitude cone electroretinograms in retinitis pigmentosa. *Am J Ophthalmol*. 1988;105:500-503.
15. Birch DG, Sandberg MA. Submicrovolt full-field cone electroretinograms: artifacts and reproducibility. *Doc Ophthalmol*. 1996;92:269-280.
16. Sutter EE. The fast m-transform: a fast computation of cross-correlations with binary m-sequences. *Soc Ind Appl Math*. 1991;20:686-694.
17. Sutter EE, Tran D. The field topography of ERG components in man-I. The photopic luminance response. *Vision Res*. 1992;32:433-446.
18. Seeliger M, Kretschmann U, Apfelstedt-Sylla E, Ruther K, Zrenner E. Multifocal electroretinography in retinitis pigmentosa. *Am J Ophthalmol*. 1998;125:214-226.
19. Hood DC, Holopigian K, Greenstein V, et al. Assessment of local retinal function in patients with retinitis pigmentosa using the multi-focal ERG technique. *Vision Res*. 1998;38:163-179.
20. Seeliger MW, Zrenner E, Apfelstedt-Sylla E, Jaissle GB. Identification of Usher syndrome subtypes by ERG implicit time. *Invest Ophthalmol Vis Sci*. 2001;42:3066-3071.
21. Chan HL, Brown B. Investigation of retinitis pigmentosa using the multifocal electroretinogram. *Ophthalmic Physiol Opt*. 1998;18:335-350.
22. Feliuss J, Swanson WH. Photopic temporal processing in retinitis pigmentosa. *Invest Ophthalmol Vis Sci*. 1999;40:2932-2944.
23. Granse L, Ponjavic V, Andreasson S. Full-field ERG, multifocal ERG and multifocal VEP in patients with retinitis pigmentosa and residual central visual fields. *Acta Ophthalmol Scand*. 2004;82:701-706.
24. Greenstein VC, Holopigian K, Seiple W, Carr RE, Hood DC. Atypical multifocal ERG responses in patients with diseases affecting the photoreceptors. *Vision Res*. 2004;44:2867-2874.
25. Fishman GA, Jacobson SG, Alexander KR, et al. Outcome measures and their application in clinical trials for retinal degenerative diseases: outline, review, and perspective. *Retina*. 2005;25:772-777.
26. Marmor MF, Holder GE, Seeliger MW, Yamamoto S. Standard for clinical electroretinography: 2004 update. *Doc Ophthalmol*. 2004;108:107-114.
27. Kawabata H, Adachi-Usami E. Multifocal electroretinogram in myopia. *Invest Ophthalmol Vis Sci*. 1997;38:2844-2851.
28. Ferris FL 3rd, Kassoff A, Bresnick GH, Bailey I. New visual acuity charts for clinical research. *Am J Ophthalmol*. 1982;94:91-96.
29. Pelli DG, Robson JG, Wilkins AJ. The design of new letter chart for measuring contrast sensitivity. *Clin Vis Sci*. 1988;2:187-199.
30. Marmor MF, Hood DC, Keating D, Kondo M, Seeliger MW, Miyake Y. Guidelines for basic multifocal electroretinography (mfERG). *Doc Ophthalmol*. 2003;106:105-115.
31. Hood DC, Li J. A technique for measuring individual multifocal ERG records. *Trends Opt Photon Opt Soc Am*. 1997;11:33-41.
32. Team RDC. *R: A Language and Environment for Statistical Computing*. Vienna, Austria: R Foundation for Statistical Computing; 2005.
33. Woody CD. Characterization of an adaptive filter for the analysis of variable latency neuroelectric signals. *Med Biol Eng*. 1967:539-553.
34. Seiple W, Clemens CJ, Greenstein VC, Carr RE, Holopigian K. Test-retest reliability of the multifocal electroretinogram and Humphrey visual fields in patients with retinitis pigmentosa. *Doc Ophthalmol*. 2004;109:255-272.

APPENDIX

Estimation of Recording Quality

Processed data were exported from unfiltered trace plots of a high-order kernel (4-2-0; epoch 0-60 ms) from VERIS. The RMS (power estimate) was calculated as follows:

$$\text{Noise} = \sum_{b=1}^{b=103} \sqrt{\frac{\sum_{i=1}^n x_i^2}{n}}$$

where b is the hexagon number and i is the sample.

Waveforms were rejected when: noise > mean noise_{controls} + 2 SD Noise_{controls} (i.e., when estimated noise exceeded the 95th percentile of our control dataset).

Identification of Hexagons with Signals

Processed data were exported from unfiltered trace plots of a first-order kernel (epoch 0-180 ms) from VERIS.

For each hexagon, RMS_{signal} (epoch 0-60 ms) and RMS_{noise} (120-180 ms) were calculated.

$$\text{RMS}_b = \sqrt{\frac{\sum_{i=1}^n x_i^2}{n}}$$

$$\text{SNR}_b = \frac{\text{RMS}_{\text{signal}_b}}{\text{RMS}_{\text{noise}_b}}$$

Hexagons were identified to contain a signal when

$$\text{SNR}_{b=1}^{b=103} + 2 \cdot \sigma_{\text{SNR}_{b=1}^{b=103}} \leq \text{SNR}_b$$